Imaging the lower limb network in Parkinson's disease

Jae Woo Chung [a], Abigail E. Bower [a], Ibrahim Malik [b], Justin P. Martello [c],
Christopher A. Knight [a,d], John J. Jeka [a,d], Roxana G. Burciu [a,d,*]

[a] Department of Kinesiology and Applied Physiology, University of Delaware, Newark, DE, United States
[b] Center for Biomedical & Brain Imaging, University of Delaware, Newark, DE, United States
[c] Department of Neurosciences, Christiana Care Health System, Newark, DE, United States
[d] Interdisciplinary Neuroscience Graduate Program, University of Delaware, Newark, DE, United States

ABSTRACT

Background: Despite the significant impact of lower limb symptoms on everyday life activities in Parkinson's disease (PD), knowledge of the neural correlates of lower limb deficits is limited.
Objective: We ran an fMRI study to investigate the neural correlates of lower limb movements in individuals with and without PD.
Methods: Participants included 24 PD and 21 older adults who were scanned while performing a precisely controlled isometric force generation task by dorsiflexing their ankle. A novel MRI-compatible ankle dorsiflexion device that limits head motion during motor tasks was used. The PD were tested on their more affected side, whereas the side in controls was randomized. Importantly, PD were tested in the off-state, following overnight withdrawal from antiparkinsonian medication.
Results: The foot task revealed extensive functional brain changes in PD compared to controls, with reduced fMRI signal during ankle dorsiflexion within the contralateral putamen and M1 foot area, and ipsilateral cerebellum. The activity of M1 foot area was negatively correlated with the severity of foot symptoms based on the Movement Disorder Society-Sponsored Revision of the Unified Parkinson's Disease Rating Scale (MDS-UPDRS-III).
Conclusion: Overall, current findings provide new evidence of brain changes underlying motor symptoms in PD. Our results suggest that pathophysiology of lower limb symptoms in PD appears to involve both the cortico-basal ganglia and cortico-cerebellar motor circuits.

1. Introduction

While the pathophysiology of Parkinson's disease (PD) is not fully understood, it has been traditionally linked to a reduction in the dopamine available to brain regions involved in motor control (Alexander, 2004; Brooks, 2010; Fahn, 2008; Meder et al., 2019; Obeso et al., 2017; Poewe et al., 2017). It is important to note that much of what is known about the neural bases of motor deficits in PD is based on task-based functional magnetic resonance imaging (fMRI) studies showing abnormal motor-related blood oxygen level dependent (BOLD) activation patterns in PD compared to healthy older adults (Burciu and Vaillancourt, 2018; Herz et al., 2014; Herz et al., 2021; Niethammer et al.,

2012). A recent coordinate-based *meta*-analysis of functional neuroimaging studies testing limb movements in PD and healthy individuals revealed consistent hypoactivation of the posterior putamen and cerebellum in PD compared to controls during a variety of motor tasks (Herz et al., 2021). The primary motor cortex (M1) and the supplementary motor area (SMA) also showed a lower degree of activation in PD across multiple studies, whereas areas localized anterior to these structures were found to be hyperactive (Herz et al., 2021).

While the imaging research carried out to date in PD points to functional abnormalities along distinct neural pathways, it is important to note that most imaging studies in PD are upper limb studies. Despite the significant impact of lower limb symptoms on everyday life activities

in PD, the neural correlates of lower limb deficits have received little attention. This knowledge is limited in part by the technical difficulties in performing controlled experiments with currently available fMRI methods. First and foremost, head motion is known to have a substantial impact on the results of fMRI studies (Friston et al., 1996; Power et al., 2012), and movements of the feet in a supine position could lead to greater disruption of the fMRI signal than movements of the hands. Of note, the coordinate-based *meta*-analysis cited above, upon the application of strict exclusion criteria, identified only two studies involving movement execution in the lower limb in PD out of thirty-nine functional studies (Herz et al., 2021). Recently, studies focusing on unique PD phenotypes (PD with freezing of gait or PD with postural instability and gait disturbances) have emerged, emphasizing the need for better understanding of lower limb deficits in PD (Agosta et al., 2017; de Lima-Pardini et al., 2017; Gilat et al., 2019; Matar et al., 2019; Piramide et al., 2020; Sarasso et al., 2021; Shine et al., 2013).

Due to differences in the tasks employed, PD phenotypes tested, as well as the relatively small number of participants in some studies, there is no clear consensus regarding the functional brain changes associated with lower limb dysfunction in PD has not been reached yet (Agosta et al., 2017; de Lima-Pardini et al., 2017; Drucker et al., 2019; Gilat et al., 2019; Katschnig et al., 2011; Matar et al., 2019; Piramide et al., 2020; Sarasso et al., 2021; Shine et al., 2013). Some results point to a reduction in activation of the striatum and sensorimotor regions, whereas other results indicate an excess of activation in premotor regions such as the SMA, pre-SMA, frontal areas and specific subdivisions of the cerebellum (Drucker et al., 2019; Katschnig et al., 2011; Piramide et al., 2020; Sarasso et al., 2021; Shine et al., 2013). Together, disparate results point to a major need to conduct more lower limb studies in PD to better understand the pathophysiology of lower limb symptoms in this population. Equally important is the need to increase the validity of research studies by additionally accounting for task performance. Parameters such as the amplitude of movements or the number of iterations can vary between PD and controls, which may account for reported differences in activation patterns.

Given that knowledge about the effect of PD on the neural circuits controlling lower limb movements is limited, the purpose of this fMRI study was to further investigate the neural correlates of lower limb function in PD vs. healthy older adults by using 1) a novel MRI-compatible ankle dorsiflexion device that produces minimal head motion and 2) a force control paradigm highly sensitive to PD deficits We administered a well-established PD force paradigm (Burciu et al., 2016a; Burciu et al., 2016b; Burciu et al., 2015; Chung et al., 2018; Neely et al., 2015; Planetta et al., 2015; Prodoehl et al., 2010; Spraker et al., 2010) to characterize and compare the fMRI correlates of lower limb function in PD and a group of matched older adults. We hypothesized that both the cortico-basal ganglia and cortico-cerebellar motor circuits will be hypoactive in PD compared to healthy older adults.

2. Methods

2.1. Participants and clinical assessments

Twenty-four PD and twenty-one healthy older adults completed this study. PD participants were diagnosed by a movement disorder specialist using established criteria (i.e., United Kingdom PD Society Brain Bank Criteria) and were recruited either from the Christiana Care Neurology Specialists Clinic in Newark, Delaware, or the University of Delaware Participant Recruitment Registry for Parkinson's Disease Research. PD patients were excluded if they had: concurrent movement disorders (e.g., dystonia), an atypical form of parkinsonism, dementia, neuropsychiatric disorders, musculoskeletal disorders, a history of cancer that required chemotherapy and/or radiotherapy or have undergone deep brain stimulation surgery for the treatment of PD symptoms. T2-weighted MRI scans were also collected as part of this study for the purpose of excluding secondary causes of parkinsonism/other

pathophysiology (e.g., vascular lesions, demyelinating lesions, tumors, etc.). Upon inspection of the MRI scans, no participant was excluded from the analysis. The older adults in the control group were recruited via advertisements in the Newark area and reported no history of neurological or neuropsychiatric disorders. Of note, PD and controls were matched at the group level for age, sex, cognitive status, and tested side (Table 1). PD participants were tested on their more affected side which could be either the dominant or non-dominant side. The tested side in controls was randomized so that there were no statistically significant group differences in the ratio of people tested on their left/right side or dominant/non-dominant side. Importantly, all testing occurred in the morning, with PD patients being tested following an overnight withdrawal from antiparkinsonian medication (~12 h after the last dose of PD medication). The Montreal Cognitive Assessment Test (MOCA) (Nasreddine et al., 2005) was used to screen for cognitive impairment, and the motor section of the Movement Disorder Society Unified Parkinson's Disease Rating Scale (MDS-UPDRS-III) (Goetz et al., 2008) was administered to assess disease severity in PD and to rule out motor symptoms in control participants. The items from the MDS-UPDRS-III

Table 1
The table lists the sociodemographics, clinical characteristics and several behavioral measures for controls and PD. The last column lists the *p*-values corresponding to the statistical analyses described in manuscript. Data represent the count or mean ± 1 standard deviation. Ranges are listed in square brackets. Of note, all tests were completed by the PD patients in the "off" state, following an overnight withdrawal from PD medication. Disease duration is defined as time since diagnosis. Abbreviations: H & Y = Hoehn and Yahr Staging Scale; LEDD = levodopa equivalent daily dose; MDS-UPDRS-III = the motor section of the Movement Disorder Society Unified Parkinson's Disease Rating Scale; Min = minute; MVC = maximum voluntary contraction; N = Newtons.; PDQ-39 = Parkinson's Disease Questionnaire – 39.

Clinical Variables	Healthy Controls	Parkinson's Disease	P-Value
N	21	24	n/a
Age (Years)	63.71 (±8.30), [50–77]	67.33 (±8.38), [49–82]	0.154
Sex (Male │ Female)	8 │ 13	12 │ 12	0.423
Handedness (Left │ Right)	8 │ 13	12 │ 12	0.175
Tested Side/Foot (Left │ Right)	8 │ 13	14 │ 10	0.175
Tested Side/Foot (Dominant │ Non-Dominant)	12 │ 9	12 │ 12	0.632
H & Y Stage	n/a	1.88 (±0.61), [1–3]	n/a
More Affected Side (Left │ Right)	n/a	14 │ 10	n/a
Disease Duration (Months Since Diagnosis)	n/a	54.92 (±41.56), [2–156]	n/a
Total LEDD	n/a	470.63 (±368.27), [60–1100]	n/a
Non-Motor Measures			
Education Level (Years)	16.63 (±2.33), [12–22]	17.58 (±2.56), [14–24]	0.221
Montreal Cognitive Assessment Test	27.48 (±2.46), [22–30]	26.75 (±2.38), [22–30]	0.279
Beck Depression Inventory – II	5.52 (±6.29), [0–24]	8.35 (±4.98), [2–19]	0.225
PDQ-39 Summary Index	n/a	17.14 (±9.67), [4–39]	n/a
Motor Measures			
MVC Tested Foot (N)	64.00 (±39.58), [15–154]	50.79 (±38.62), [12–171]	0.210
MDS-UPDRS-III – Total Score	1.95 (±3.17), [0–11]	32.21 (±11.10), [13–56]	< 0.001
MDS-UPDRS-III – Tested Foot	0.10 (±0.30), [0–1]	4.08 (±2.41), [0–9]	< 0.001
MDS-UPDRS-III – Other Foot	0.24 (±0.62), [0–2]	2.92 (±2.16), [0–2]	< 0.001

assessing toe taps and leg lifts were summed up to characterize the severity of the PD symptoms in the tested vs. other foot. As one can see in Table 1, the foot score was greater for the foot tested inside the MRI scanner than for the other foot. Mood and quality of life were evaluated with the Beck Depression Inventory-II (BDI) and the 39-item Parkinson's Disease Questionnaire (PDQ-39) (Jenkinson et al., 1997; Upton, 2013) (Table 1). Written informed consent was obtained from all participants in the study. Testing procedures were approved by the local Institutional Review Board and conducted according to the Declaration of Helsinki.

2.2. Force data acquisition

Participants completed a force control task while laying supine on the MRI bed. A custom-made MRI-compatible device and a fiber-optic force transducer that could measure up to 700 N were used (Neuroimaging Solutions, Gainesville, FL) (Fig. 1A). We stabilized the participant's tested foot with an adjustable strap placed over the metatarsals. By fixating the foot and using an isometric force task we minimized the head motion which is usually higher when performing tasks that involve the lower limb vs. the upper limb. Small cushions were placed around the participant's head to further minimize head motion during data collection. To ensure comfort during the MRI procedure, a small cushion was placed under the knee. Each time a participant dorsiflexed the ankle, a piston at the back of the foot device applied compressive force to the force sensor. Online visual feedback of the force output was projected onto a 32″ 1920 × 1080 widescreen LCD display with a 120 Hz refresh rate located behind the MRI bore/participant's head. The display

was visible to participants via a mirror mounted on the head coil. Force signals were transmitted through a fiber-optic cable to a SI155 Micron Hyperion Optical Sensing Interrogator (Micron Optics, Atlanta, Georgia) which digitized the force data. Force data were collected using custom software written in LabVIEW (National Instruments, Austin, TX).

2.3. Force paradigm and experimental procedures

First, for each participant, we measured the maximum voluntary contraction (MVC) of the tested foot. A change in color from red to green of a horizontal bar visible on the screen instructed participants to dorsiflex their ankle and produce maximum force. The average peak force from three 5-s trials was used to normalize force demands across participants to be 15% of their MVC. A representation of the fMRI paradigm is shown in Fig. 1B. Each task began with a 30-s rest block followed by four cycles of 30-s of force alternating with 30 s of rest. Each of the four force blocks consisted of 10 trials. During the force task, two horizontal bars were displayed on the screen. The top bar was white, stationary, and represented the target set at 15 % of MVC. The bottom bar represented the participant's force, it was colored and could move up and down the screen based on the amount of force produced by the participant. Force generation was visually cued by a change in color of the force bar. When the force bar was red (for 1 s), participants relaxed, and when the force bar was green (for 2 s), participants had to generate force. Instructions were to be quick in generating the force, produce enough force to bring the green bar on top of the white bar, and then relax/produce no force while the bar was red. The choice to provide
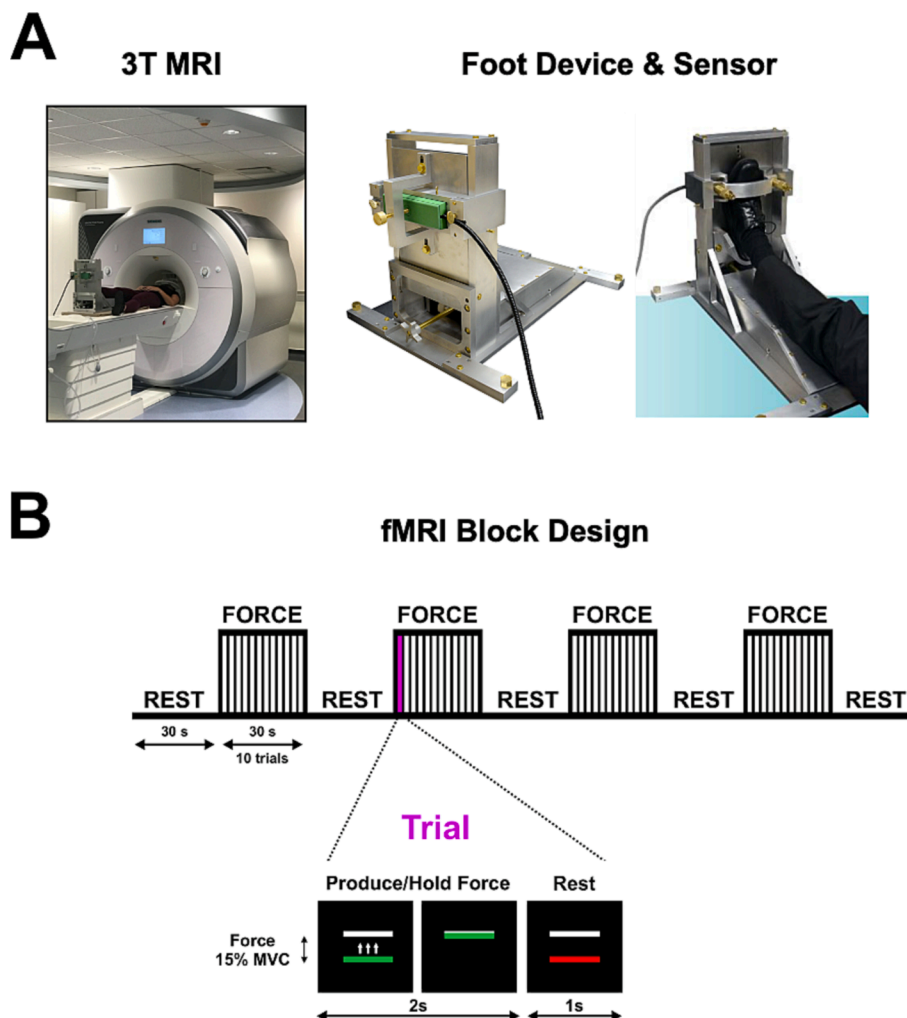

Fig. 1. Experimental setup and fMRI paradigm. (A) Custom-designed MRI compatible foot device placed on the MRI table along with pictures of the foot sensor used for the force production task. During the foot task, participants produced force by dorsiflexing the ankle. The tested side was the more affected side in PD and either the left or the right in controls (testing side was randomized in the control group; see Table 1). (B) fMRI paradigm. A block design was used. The foot task began with 30 s of rest, followed by 4 cycles consisting for 30 s force + 30 s rest. Each of the four force blocks contained 10 trials. During a trial, participants had to produce force for 2 s and relax for 1 s. A white bar represented their target and was set to be 15% of the effector/limb's maximum voluntary contraction (MVC). Force generation was cued by a change in color of a force bar. When the force bar located at the bottom of the screen turned green, participants dorsiflexed their ankle to bring the force bar on top of a white bar (i.e., produce force). When the force bar located at the bottom of the screen turned red, participants relaxed their ankle to bring down the force bar to the bottom of the screen. (For interpretation of the references to color in this figure legend, the reader is referred to the web version of this article.)

online feedback on performance was motivated by the need to ensure that one group is not producing more force than the other, which would have major implications for the interpretation of any group differences in the fMRI activity. Importantly, all participants completed a training session prior to beginning data collection to make sure the instructions were clear and to prevent a possible learning effect while in the scanner.

2.4. Force data analysis

The force data collected inside the MRI was inspected in real time while participants were inside the MRI scanner to make sure participants followed the instructions and produced 10 trials per block. The analysis of the force data was performed using custom scripts in MATLAB R2021b (The Mathworks, Natick, MA). First, data were filtered using a 6th-order Butterworth filter with a cutoff frequency of 15 Hz. Next, for each force trial, the following time points were manually marked: 1) the onset of the steady period and 2) the offset of the steady period. These two time points were used to calculate the following force parameters: a) average force amplitude during the steady period and b) the standard deviation (SD) of force produced during the stead period (both measures expressed as % of MVC). We hypothesized that these measures, which could in some cases have an influence on the fMRI signal, would not differ between PD and controls.

2.5. MRI data acquisition

MRI images were collected at the University of Delaware's Center for Biomedical and Brain Imaging, on a 3 T Magnetom Prisma whole-body MRI scanner from Siemens equipped with a 64-channel head coil. Functional MRI data were collected using a single-shot gradient echo-planar imaging pulse sequence (TR = 2500 ms, TE = 30 ms, 43 slices, flip angle = 80°, GRAPPA parallel imaging factor 2, FOV = 240 × 240 mm, resolution = 3 × 3 × 3 mm). A total of 108 TRs were collected. High-resolution structural MRI scans were collected using a T1-weighted sequence (TR = 2000 ms, TE = 2.99 ms, 208 slices, flip angle = 8°, GRAPPA parallel imaging factor 2, FOV = 256 × 256 mm, resolution = 0.8 × 0.8 × 0.8 mm). T2-weighted scans were also collected (TR = 2500 ms, TE = 371 ms, 208 slices, flip angle = variable, GRAPPA parallel imaging factor 3, FOV = 256 × 256 mm, resolution = 0.8 × 0.8 × 0.8 mm).

2.6. MRI data analysis

2.6.1. Functional MRI

2.6.1.1. Single-subject and group-level analyses. Quality assessments were performed on all MRI scans. Consistent with previous research testing unilateral movements (Burciu et al., 2016a; Burciu et al., 2015; Chung et al., 2018; Planetta et al., 2015; Spraker et al., 2010), the fMRI and T1-weighted scans of participants who were tested on their left side were flipped in the left–right plane prior to processing. Thus, in the results section we refer to the left side of the brain images as contralateral to the foot producing force and the right side as ipsilateral to the foot producing force. The fMRI data were analyzed using several MRI software packages including AFNI (Analysis of Functional Neuro Images; https://afni.nimh.nih.gov), SPM12 (Statistical Parametric Mapping, https://www.fil.ion.ucl.ac.uk/spm/), as well as custom UNIX shell scripts. The fMRI analysis consisted of the following preprocessing steps: 1) skullstripping the T1-weighted scan, 2) despiking the fMRI scan to remove extreme time series outliers, 3) slice-timing correction of the fMRI scan for interleaved acquisition, 4) 3D rigid-body motion correction of the fMRI scan, 5) motion scrubbing by removing TR-to-TR motion > 0.5 mm, 6) coregistration of the fMRI and T1-weighted scans, 7) division of the fMRI signal in each voxel at each point in the time series by the mean signal in that voxel across the scan, 8) spatial normalization

of the scans to the 152MNI template for a standard whole-brain analysis and to the SUIT template (Spatially Unbiased Infratentorial Template; https://www.diedrichsenlab.org/imaging/suit.htm) for a cerebellum- and brainstem-optimized analysis (Diedrichsen, 2006), 9) smoothing of the spatially normalized fMRI scans with a 4-mm Full Width Half Max (FWHM) Gaussian kernel to account for inter-subject variability in brain anatomy in the group-level analyses. Following preprocessing, the fMRI signal during the four 30-s force blocks was modeled using a boxcar regressor convolved with the canonical hemodynamic response function. The six head motion parameters estimated during the 3D rigid-body motion correction were included in the statistical analysis as regressors of no interest. The dependent variable at this level of the analysis was the estimated β-coefficient of the regressed time series and its associated t-statistic. Finally, we performed a voxel-wise Independent T-Test analysis to compare foot-related activity between PD and controls. The analysis was corrected for Type I error using a Monte Carlo simulation using 3dClustSim in AFNI. Active regions had to meet a threshold of p < 0.001 and a cluster size of 54 μL, corresponding to a p < 0.05, corrected for multiple comparisons using the family-wise error (FWE) correction. Significant group differences were labeled using the basal ganglia human area template (BGHAT), the human motor area template (HMAT), the probabilistic atlas of the human cerebellum (SUIT), and the automated anatomical labeling atlas (AAL) (Diedrichsen et al., 2009; Mayka et al., 2006; Prodoehl et al., 2008; Tzourio-Mazoyer et al., 2002).

2.6.1.2. Correlations between BOLD fMRI percent signal change and disease severity. Percent signal change (PSC) was calculated from the motor regions where fMRI activity differed between groups and correlated in PD with disease severity expressed as the total MDS-UPDRS-III and the MDS-UPDRS-III subscore corresponding to the tested foot. PSC was calculated for a 15-s period spanning 6TRs at the end of each force block based on previous force control studies in PD (Burciu et al., 2016a; Chung et al., 2018; Spraker et al., 2010). The relation between fMRI activity and disease severity was assessed with Spearman correlations set at a p < 0.05.

2.6.1.3. Volume of fMRI activation. The mean activity maps for the PD and control groups derived from the voxel-wise statistical analysis were binarized such that significantly active voxels were assigned a value of 1 and all other voxels were assigned a value of zero. The three atlases corresponding to the main nodes of the motor circuit (basal ganglia – BGHAT, cortical motor regions – HMAT, and cerebellum – SUIT were also binarized and used to mask the mean activity map for each group. The total number of active voxels within the basal ganglia, cortical motor areas, and cerebellum was normalized by the size of the atlas and plotted for each group.

2.6.2. Structural MRI

The T1-weighted scans were submitted to a voxel-based morphometry analysis (VBM). This analysis was performed with the purpose of determining if the functional brain changes in PD resulting from the fMRI analysis are accompanied by structural changes of the gray matter. The VBM analysis was conducted using the CAT12 toolbox (Computational Anatomy Toolbox, https://neuro-jena.github.io/cat/) in SPM12 (Statistical Parametric Mapping, https://www.fil.ion.ucl.ac.uk/spm/), which in turn ran in MATLAB R2021b (The Mathworks, Natick, MA). Scans were corrected for signal inhomogeneities and segmented into three tissue classes: gray matter (GM), white matter (WM), and cerebrospinal fluid (CSF). The GM maps were spatially normalized using the Diffeomorphic Anatomic Registration Through Exponentiated Lie algebra algorithm (DARTEL) to the MNI space for a standard whole-brain analysis (Ashburner, 2007), and to the SUIT template for a cerebellum- and brainstem-optimized analysis. Following spatial normalization, GM maps were modulated using the Jacobian determinant maps

to retain pre-normalization volume information, and smoothed with an 8-mm FWHM Gaussian kernel for the whole-brain analysis and a 4-mm kernel for the cerebellum- and brainstem-optimized analysis. To compare gray matter volume between PD and controls, a GLM analysis was set up with total intracranial volume (TIV) as a covariate. Statistical significance was determined using conventional methods available in SPM12 (i.e., $p < 0.05$, corrected for multiple comparisons using the FWE correction).

2.7. Statistical analysis

Statistical analyses of non-imaging data were performed in SPSS 28.0 (IBM, New York). Prior to performing any of these statistical analyses, outcome measures were assessed for normality and equal variance with the Shapiro-Wilk and Levene's Tests. The results of these tests prompted the choice of parametric or non-parametric statistical testing. Categorical data (i.e., sex, tested side based on body side or dominance; Table 1) were compared between groups using a Chi-Square test. All continuous measures except for age were compared between groups using the Mann-Whitney U Test. Age differences were compared using an Independent T-Test. Correlation analyses in PD between the fMRI activity extracted from motor regions where group differences were found and the severity of motor symptoms based on the MDS-UPDRS-III scores were evaluated with Spearman correlations. Results were significant if $p < 0.05$.

3. Results

3.1. Clinical and force measures

There were no significant differences between groups in age, sex, tested side based on body side (left vs. right) or dominance (dominant vs. non-dominant), education level, cognitive status, and depression score (p values > 0.05; Table 1). As expected, group differences were found in the total MDS-UPDRS-III score and the MDS-UPDRS-III subscores for the tested foot and other foot (p values < 0.001; Table 1). There were no differences between groups in the MVC ($p = 0.210$). As for the force measures, there were no significant differences between groups in the normalized force amplitude during the steady period ($p = 0.720$; mean force controls $= 15.00 \pm 2.87$, mean force PD $= 13.47 \pm 2.02$) or force variability measured as the SD of the force produced during the steady period ($p = 0.539$; mean SD controls $= 1.37 \pm 0.62$, mean SD PD $= 1.31 \pm 0.50$).

3.2. fMRI results

Importantly, the head motion averages across the three planes did not differ between groups ($p = 0.909$; controls $= 0.09$ mm ± 0.04 mm, PD $= 0.10$ mm ± 0.06 mm). The number of TRs included in the voxel-wise fMRI analysis following the head motion scrubbing procedure also did not differ between groups ($p = 0.235$; maximum TRs per task $= 108$; controls $= 103.95 \pm 5.41$, PD $= 103.54 \pm 8.77$).

Fig. 2 shows the mean fMRI activity for controls and PD. In controls, the performance of the ankle dorsiflexion task resulted in robust activation of the basal ganglia, motor and premotor cortices, thalamus, and cerebellum. In PD, the task engaged the same brain regions but to a lesser extent. The voxel-wise statistical analysis revealed an extensive pattern of hypoactivation in PD compared to controls in the contralateral posterior putamen, contralateral M1 foot area, contralateral thalamus, ipsilateral caudate, and the temporal and occipital cortices bilaterally (Fig. 3A, Table 2). In the cerebellum, PD had reduced motor-related activity compared to controls in the ipsilateral lobules I-VI, ipsilateral deep cerebellar nuclei including the dentate nucleus, ipsilateral lobules VIIIa-b, IX, and Crus I, and vermis VIIIa-b (Fig. 3A, Table 2).

Spearman correlations were run between total MDS-UPDRS-III/MDS-UPDRS-III subscore for the tested foot and the PSC in the
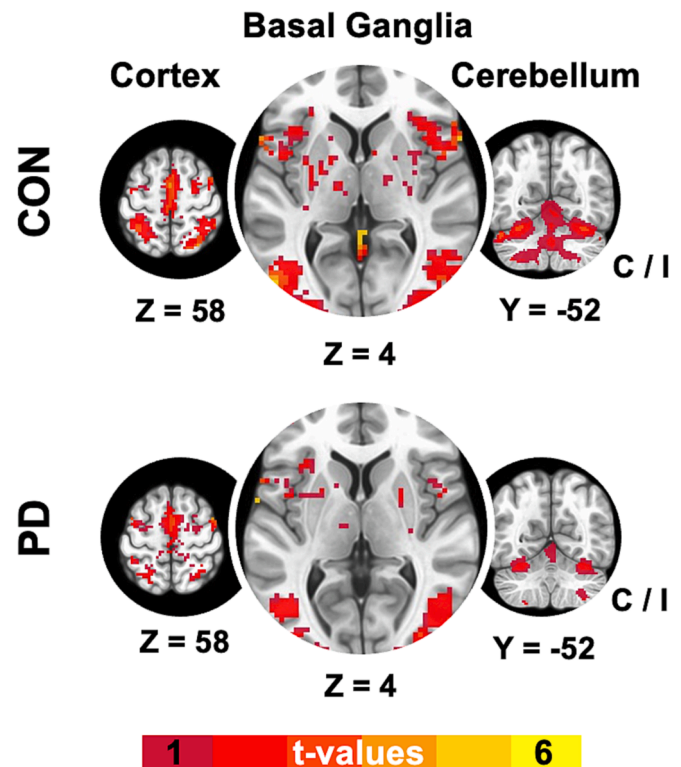

Fig. 2. The figure illustrates the results of the whole-brain and cerebellum/brainstem-optimized analyses. Data represent the mean fMRI activity during the ankle dorsiflexion task for the PD and control groups. Brain data is overlaid on the MNI template. The color bars indicate the intensity of the fMRI results in t-values.

contralateral posterior putamen, contralateral M1 foot area, and the largest ipsilateral cluster in the cerebellum spanning lobule IX, vermis VIIIa/b/IX, and the deep cerebellar nuclei. We found a negative correlation between PSC during the foot task in contralateral M1 foot area and total MDS-UPDRS-III (rho $= -0.517$, $p = 0.010$) and between M1 foot area and the MDS-UPDRS-III subscore for the tested foot (rho $= -0.475$, $p = 0.019$) (Fig. 3B). No other correlations were detected (p values > 0.05).

The intersection of the mean activity maps for controls and PD with the motor atlases resulted in a normalized activation volume per motor node (Fig. 4). While this analysis is exploratory and does not represent the main focus of this study (limitations are being addressed in the discussion), it suggests that a large portion of the cerebellum is engaged by the foot task compared to the basal ganglia and cortical motor areas.

3.3. VBM results

No significant differences in GM volume were found between PD and controls.

4. Discussion

The results of this study contribute to the PD literature in several ways. First, we revealed an extensive pattern of hypoactivity during ankle dorsiflexion in PD compared to controls that encompasses the primary nodes of the motor circuit: basal ganglia, cerebellum, and M1. Second, our results showed that the fMRI activity within the M1 foot area was markedly lower in those PD exhibiting more severe symptoms based on the clinical examination.

While the functional activation profile for upper limb motor control in PD has been widely explored using various paradigms (Burciu et al., 2015; Eckert et al., 2006; Herz et al., 2014; Herz et al., 2021; Kraft et al.,
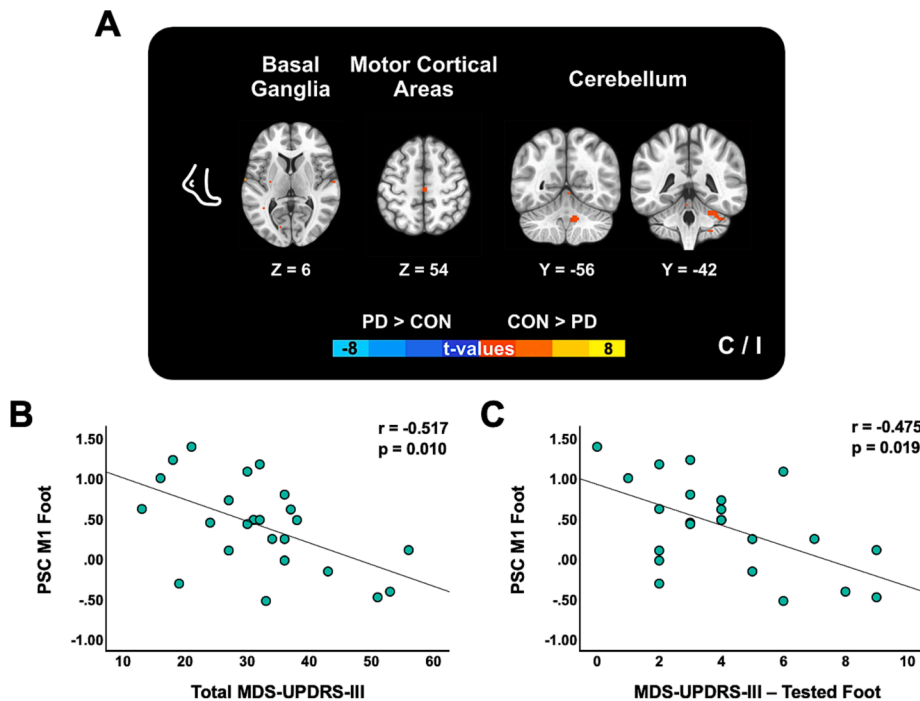
Fig. 3. (A) The figure depicts group differences in the fMRI activation during the ankle dorsiflexion task. The color scale uses warm colors for depicting brain regions where controls have greater activity than PD. Blue colors are used for any region where brain activity is greater in PD than in controls. Results are overlaid on the MNI template. Regions displaying activation had to meet a threshold of $p < 0.001$ and a cluster size of 54 μL, corresponding to a $p < 0.05$, corrected for multiple comparisons using the family-wise error (FWE) correction. (B) Correlation plots illustrating the relation in PD between PSC in the contralateral M1 foot area during the foot task and the severity of the disease expressed as the total MDS-UPDRS-III score and MDS-UPDRS-III subscore for the tested/more affected foot. Abbreviations: C = contralateral to the foot producing force; I = ipsilateral to the foot producing force; M1 = primary motor cortex; MDS-UPDRS-III = the motor section of the Movement Disorder Society Unified Parkinson's Disease Rating Scale; PSC = percent signal change. (For interpretation of the references to color in this figure legend, the reader is referred to the web version of this article.)

Table 2

The table describes fMRI results in terms of anatomical location, side of activation, cluster size, and intensity (t-value). Only brain regions surviving a height threshold of $p < 0.001$ (cluster size correction using 3dClustSim in AFNI providing an FWE-corrected $p < 0.05$). MNI coordinates for the voxel with the highest intensity in each cluster are provided. Abbreviations: C = contralateral to the foot producing force; I = ipsilateral to the foot producing force; MNI = Montreal Neurological Institute.

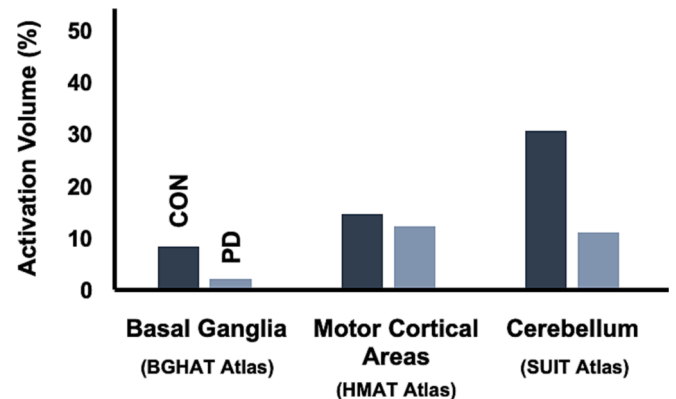| Anatomical Regions	Side	Cluster Size (μL)	Peak X Y Z MNI Coordinates	T-Value
Healthy Controls > Parkinson's Disease				
Primary motor cortex (foot area)	C	351	−2, −22, 54	4.08
Posterior putamen	C	54	−30, −12, 6	3.33
Caudate	I	54	12, 14, 0	3.37
Cerebellum: lobule IX, vermis VIIIa/b/IX; deep cerebellar nuclei: dorsal/motor dentate, fastigial, interposed	I	664	10, −54, −36	4.86
Cerebellum: lobules I-IV (foot area), V, VI, Crus I	I	632	28, −38, −26	3.63
Cerebellum: lobule VI	I	264	26, −68, −20	3.90
Cerebellum: lobule VIIIb	I	160	28, −42, −50	3.41
Cerebellum: lobules I-IV,V	I	144	2, −54, −4	3.78
Cerebellum: vermis VIIIa	I	40	2, −70, −44	3.47
Cerebellum: lobule VIIIb	C	160	−22, −52, −46	3.93
Thalamus	C	162	−12, −12, 8	3.32
Thalamus	C	108	−4, −6, 2	3.46
Lingual gyrus	C	243	−4, −66, 0	4.24
Calcarine gyrus	C	189	−16, −78, 6	3.73
Superior temporal gyrus	I	270	68, −36, 14	3.47
Insula	I	324	42, −4, −10	3.32
Superior occipital gyrus	C	216	−12, −88, 8	3.79
Superior occipital gyrus	I	162	26, −88, 12	3.49
Superior temporal gyrus	C	162	−64, −24, 12	3.43
Parkinson's Disease > Healthy Controls				
–		–	–	–

Fig. 4. The figure depicts the normalized activation volume for each group, calculated for the main nodes of the motor circuit (i.e., basal ganglia, cortical motor regions and cerebellum). Values were obtained by masking the mean activity maps for each group derived from the voxel-wise statistical analyses with the following atlases: BGHAT, HMAT, and SUIT. The total number of active voxels was normalized by the size of the atlas. Results should be interpreted with caution due to the lack of a statistical analysis.

2009; Martin et al., 2019; Pinto et al., 2011; Prodoehl et al., 2010; Sabatini et al., 2000; Spraker et al., 2010; Wu et al., 2010), the same is not true for lower limb control. Here, the current ankle dorsiflexion task revealed a significant change in force-related fMRI activity in PD (i.e., hypoactivation) that encompass all the primary nodes of the motor network: basal ganglia, M1 and cerebellum. It is important to note that these results were found in the absence of significant head motion or group differences in head motion and performance on the force task. Reductions in the activity of basal ganglia nuclei and sensorimotor regions have been found before in heterogeneous PD groups as well as in specific PD phenotypes (e.g., PD with freezing of gait or PIGD) using either upper limb tasks, virtual reality gait paradigms or dual tasks (Herz et al., 2014; Herz et al., 2021; Matar et al., 2019; Sarasso et al., 2021; Shine et al., 2013). In a study including both active and passive ankle dorsiflexion, the SMA and pre-SMA were found to be hyperactive in PD

compared to controls (Katschnig et al., 2011). More recently, in a study that tested internally guided rhythmic foot tapping (slow, slow, quick, quick, slow tango rhythm) and externally guided rhythmic foot tapping using a tactile cue, PD had less activation in the striatum and motor cortex compared to controls (Drucker et al., 2019). Also, a task-by-group interaction was found in the cerebellum, with increased activation of the cerebellum for the internally guided condition in the PD group. A combination of hypoactivation and hyperactivation appears to be more prominent in PD phenotypes. In PD with freezing of gait for instance, there is often a decrease in activity of the basal ganglia and an increase in activity in cerebellar, fronto-parietal, or parieto-occipital areas (Agosta et al., 2017; Piramide et al., 2020; Sarasso et al., 2021).

An important aspect to consider when interpreting the different patterns of fMRI activity in both the lower limb but also the upper limb literature is motor performance. Parameters such as the force level produced during the task, the degree of dorsiflexion if the lower limb task is not isometric, variability or the number of trials could be accounting for differences in task activation, especially in repetitive tapping movements. The force task used here is instrumented, and has been widely used and validated in upper limb fMRI studies in PD (Burciu et al., 2016a; Burciu et al., 2015; Prodoehl et al., 2010; Spraker et al., 2010), and is known to control well for these potentially confounding factors. Here, in the first lower limb imaging study utilizing this well-validated isometric force control paradigm, we showed that PD performed in a similar way to controls, with no statistically significant differences between them in the amount of force produced inside the scanner or the variability of the generated force. These results strengthen the imaging findings as often, differences in task performance between a clinical cohort and healthy individuals can influence the directionality of fMRI group differences. For instance, a hypoactivity or hyperactivity pattern could be at times related to one group producing less or more force, respectively.

Taken together, the results presented in this study contribute to the existing imaging literature in PD by showing that the cortico-basal ganglia and cortico-cerebellar motor circuits are impaired not only during upper limb movements but also during lower limb movements (Burciu et al., 2016a; Burciu et al., 2015; Herz et al., 2014; Herz et al., 2021; Prodoehl et al., 2010; Spraker et al., 2010). While most imaging studies focus on the amplitude of the BOLD fMRI response as the main outcome measure, it may be useful in future studies to consider evaluating not only the magnitude of the activation but also the extent of the activation. Here, we performed a secondary exploratory analysis that calculated the normalized activation volume for the basal ganglia, cortical motor areas and cerebellum based on the intersection of the group-level mean activity maps with the BGHAT, HMAT, and SUIT atlases (Fig. 4). While this calculation has not been submitted to statistical analysis and is not considered to be the main priority of this study, it suggests that the cortico-basal ganglia and cortico-cerebellar motor circuits may be engaged to a different extent. It would seem (by visual inspection only) that a large percentage of the cerebellum was activated by the foot task in healthy older adults and not as much in PD. Although differences in activation volume across the two cortical-subcortical motor pathways could contribute to a better understanding of the lower limb activation profile in PD, such findings need to be interpreted with caution due to the lack of statistical analysis.

Importantly, while the current cross-sectional study design does not permit testing causality, on a speculative note, our group differences in fMRI activity during ankle dorsiflexion suggest that the pathophysiology of lower limb symptoms in PD possibly expands outside the nigrostriatal circuit to include the cerebellum and M1. Despite the controversial role of the cerebellum in PD (Lewis et al., 2013; Solstrand Dahlberg et al., 2020; Wu and Hallett, 2013), it is a structure with a heavy influence on the motor output (Caligiore et al., 2017; Kishore et al., 2014). There has been a continuous debate on whether the cerebellum plays a compensatory role or is part of the pathophysiology of PD. Our cerebellar findings are in line with the results of a recent coordinate-based meta-analysis that demonstrated a consistent pattern of hypoactivation of the cerebellum in PD (Herz et al., 2021). However, there are also studies in the literature that report hyperactivation of the cerebellum and support the hypothesis that the cerebellum plays a compensatory role in PD (Solstrand Dahlberg et al., 2020; Wu and Hallett, 2013). This compensatory hypothesis cannot be ruled out and may be related to a greater engagement of the cerebellum in more complex tasks that require increased cognitive demands. However, more evidence for this hypothesis is needed, ideally from longitudinal fMRI studies. As for the activity of cortical motor areas, the M1 foot area was found to be both reduced in PD and related to the severity of motor symptoms including those in the tested foot. This suggests that the functional integrity of the main brain region responsible for generating the signal to control the lower limb likely deteriorates with disease progression. A relatively recent longitudinal study in PD employing task-based fMRI during an isometric force control task found that the PD showed a decline in functional activity over the course of 1 year in the putamen and M1 compared to controls (Burciu et al., 2016a). Here, the correlation between the activity level of the M1 foot area and foot symptoms based on the MDS-UPDRS-III, together with previous findings in the hand, reinforces the theory that the pathophysiology of PD is not confined to the nigrostriatal dopaminergic pathway but propagates along the basal ganglia-thalamo-cortical neural network. Based on these collective findings it could be that non-pharmacologic interventions involving the cerebellum itself or nodes of the cerebello-thalamo-cortical pathways such M1 foot area may be desirable, particularly since the positive effect of acute levodopa was shown to be limited to the putamen and thalamus in an fMRI study involving active ankle movements (Schwingenschuh et al., 2012).

Finally, it is important to note that fMRI changes in PD were found in the absence of any structural changes in the gray matter layer as determined by VBM analysis. The VBM analysis confirms prior work in PD with normal cognition. Changes in the gray matter volume are not commonly observed in non-demented patients, with some changes occurring either in the more advanced stages of the disease or in patients with cognitive impairment (Burciu and Vaillancourt, 2018; Fioravanti et al., 2015; Pyatigorskaya et al., 2014; Sterling et al., 2016).

In conclusion, this study demonstrates extensive functional changes within the cortico-basal ganglia and cortico-cerebellar motor circuits during lower limb movements in PD but also the feasibility of a novel MRI-compatible ankle dorsiflexion apparatus in providing robust and reliable motor-related brain activity patterns with minimal head motion. The device along with the force protocol could help future longitudinal studies assessing the progression of lower limb symptoms in PD and/or responsiveness to pharmacologic and non-pharmacologic interventions.

Funding sources

CRediT authorship contribution statement

Jae Woo Chung: Investigation, Software, Formal analysis, Writing – original draft, Writing – review & editing. **Abigail E. Bower:** Investigation, Writing – review & editing. **Ibrahim Malik:** Investigation, Writing – review & editing. **Justin P. Martello:** Writing – review & editing. **Christopher A. Knight:** Writing – review & editing. **John J. Jeka:** Writing – review & editing. **Roxana G. Burciu:** Conceptualization, Methodology, Investigation, Formal analysis, Writing – original draft, Writing – review & editing.

Declaration of Competing Interest

The authors declare that they have no known competing financial interests or personal relationships that could have appeared to influence

the work reported in this paper.

Data availability

The data that has been used is confidential.

Acknowledgment

References

Agosta, F., Gatti, R., Sarasso, E., Volonté, M.A., Canu, E., Meani, A., Sarro, L., Copetti, M., Cattrysse, E., Kerckhofs, E., Comi, G., Falini, A., Filippi, M., 2017. Brain plasticity in Parkinson's disease with freezing of gait induced by action observation training. J. Neurol. 264, 88–101.

Alexander, G.E., 2004. Biology of Parkinson's disease: pathogenesis and pathophysiology of a multisystem neurodegenerative disorder. Dialogues Clin. Neurosci. 6, 259–280.

Ashburner, J., 2007. A fast diffeomorphic image registration algorithm. Neuroimage 38, 95–113.

Brooks, D.J., 2010. Imaging Approaches to Parkinson Disease. J. Nucl. Med. 51, 596.

Burciu, R.G., Ofori, E., Shukla, P., Planetta, P.J., Snyder, A.F., Li, H., Hass, C.J., Okun, M. S., McFarland, N.R., Vaillancourt, D.E., 2015. Distinct patterns of brain activity in progressive supranuclear palsy and Parkinson's disease. Mov. Disord. 1248–1258.

Burciu, R.G., Chung, J.W., Shukla, P., Ofori, E., Li, H., McFarland, N.R., Okun, M.S., Vaillancourt, D.E., 2016a. Functional MRI of disease progression in Parkinson disease and atypical parkinsonian syndromes. Neurology 87, 709–717.

Burciu, R.G., Ofori, E., Shukla, P., Pasternak, O., Chung, J.W., McFarland, N.R., Okun, M. S., Vaillancourt, D.E., 2016b. Free-water and BOLD imaging changes in Parkinson's disease patients chronically treated with a MAO-B inhibitor. Hum. Brain Mapp. 37, 2894–2903.

Burciu, R.G., Vaillancourt, D.E., 2018. Imaging of Motor Cortex Physiology in Parkinson's Disease. Mov. Disord. 33, 1688–1699.

Caligiore, D., Pezzulo, G., Baldassarre, G., Bostan, A.C., Strick, P.L., Doya, K., Helmich, R. C., Dirkx, M., Houk, J., Jörntell, H., Lago-Rodriguez, A., Galea, J.M., Miall, R.C., Popa, T., Kishore, A., Verschure, P.F.M.J., Zucca, R., Herreros, I., 2017. Consensus Paper: Towards a Systems-Level View of Cerebellar Function: the Interplay Between Cerebellum, Basal Ganglia, and Cortex. Cerebellum 16, 203–229.

Chung, J.W., Burciu, R.G., Ofori, E., Coombes, S.A., Christou, E.A., Okun, M.S., Hess, C. W., Vaillancourt, D.E., 2018. Beta-band oscillations in the supplementary motor cortex are modulated by levodopa and associated with functional activity in the basal ganglia. Neuroimage Clin. 19, 559–571.

de Lima-Pardini, A.C., de Azevedo Neto, R.M., Coelho, D.B., Boffino, C.C., Shergill, S.S., de Oliveira Souza, C., Brant, R., Barbosa, E.R., Cardoso, E.F., Teixeira, L.A., Cohen, R.G., Horak, F.B., Amaro Jr., E., 2017. An fMRI-compatible force measurement system for the evaluation of the neural correlates of step initiation. Sci. Rep. 7, 43088.

Diedrichsen, J., 2006. A spatially unbiased atlas template of the human cerebellum. Neuroimage 33, 127–138.

Diedrichsen, J., Balsters, J.H., Flavell, J., Cussans, E., Ramnani, N., 2009. A probabilistic MR atlas of the human cerebellum. Neuroimage 46, 39–46.

Drucker, J.H., Sathian, K., Crosson, B., Krishnamurthy, V., McGregor, K.M., Bozzorg, A., Gopinath, K., Krishnamurthy, L.C., Wolf, S.L., Hart, A.R., Evatt, M., Corcos, D.M., Hackney, M.E., 2019. Internally Guided Lower Limb Movement Recruits Compensatory Cerebellar Activity in People With Parkinson's Disease. Front. Neurol. 10.

Eckert, T., Peschel, T., Heinze, H.J., Rotte, M., 2006. Increased pre-SMA activation in early PD patients during simple self-initiated hand movements. J. Neurol. 253, 199–207.

Fahn, S., 2008. The history of dopamine and levodopa in the treatment of Parkinson's disease. Mov. Disord. 23 (Suppl 3), S497–S508.

Fioravanti, V., Benuzzi, F., Codeluppi, L., Contardi, S., Cavalleri, F., Nichelli, P., Valzania, F., 2015. MRI correlates of Parkinson's disease progression: a voxel based morphometry study. Parkinsons Dis. 2015, 378032.

Friston, K.J., Williams, S., Howard, R., Frackowiak, R.S.J., Turner, R., 1996. Movement-Related effects in fMRI time-series. Magn. Reson. Med. 35, 346–355.

Gilat, M., Dijkstra, B.W., D'Cruz, N., Nieuwboer, A., Lewis, S.J.G., 2019. Functional MRI to Study Gait Impairment in Parkinson's Disease: a Systematic Review and Exploratory ALE Meta-Analysis. Curr. Neurol. Neurosci. Rep. 19, 49.

Goetz, C.G., Tilley, B.C., Shaftman, S.R., Stebbins, G.T., Fahn, S., Martinez-Martin, P., Poewe, W., Sampaio, C., Stern, M.B., Dodel, R., Dubois, B., Holloway, R., Jankovic, J., Kulisevsky, J., Lang, A.E., Lees, A., Leurgans, S., LeWitt, P.A., Nyenhuis, D., Olanow, C.W., Rascol, O., Schrag, A., Teresi, J.A., van Hilten, J.J., LaPelle, N., 2008. Movement Disorder Society-sponsored revision of the Unified Parkinson's Disease Rating Scale (MDS-UPDRS): Scale presentation and clinimetric testing results. Mov. Disord. 23, 2129–2170.

Herz, D.M., Eickhoff, S.B., Løkkegaard, A., Siebner, H.R., 2014. Functional neuroimaging of motor control in parkinson's disease: A meta-analysis. Hum. Brain Mapp. 35, 3227–3237.

Herz, D.M., Meder, D., Camilleri, J.A., Eickhoff, S.B., Siebner, H.R., 2021. Brain Motor Network Changes in Parkinson's Disease: Evidence from Meta-Analytic Modeling. Mov. Disord. 36, 1180–1190.

Jenkinson, C., Fitzpatrick, R.A.Y., Peto, V.I.V., Greenhall, R., Hyman, N., 1997. The Parkinson's Disease Questionnaire (PDQ-39): development and validation of a Parkinson's disease summary index score. Age Ageing 26, 353–357.

Katschnig, P., Schwingenschuh, P., Jehna, M., Svehlík, M., Petrovic, K., Ropele, S., Zwick, E.B., Ott, E., Fazekas, F., Schmidt, R., Enzinger, C., 2011. Altered functional organization of the motor system related to ankle movements in Parkinson's disease: insights from functional MRI. J. Neural Transm. (Vienna) 118, 783–793.

Kishore, A., Meunier, S., Popa, T., 2014. Cerebellar influence on motor cortex plasticity: behavioral implications for Parkinson's disease. Front. Neurol. 5, 68.

Kraft, E., Loichinger, W., Diepers, M., Lule, D., Schwarz, J., Ludolph, A.C., Storch, A., 2009. Levodopa-induced striatal activation in Parkinson's disease: a functional MRI study. Parkinsonism Relat. Disord. 15, 558–563.

Lewis, M.M., Galley, S., Johnson, S., Stevenson, J., Huang, X., McKeown, M.J., 2013. The Role of the Cerebellum in the Pathophysiology of Parkinson's Disease. Can. J. Neurol. Sci. / Journal Canadien des Sciences Neurologiques 40, 299–306.

Martin, J.A., Zimmermann, N., Scheef, L., Jankowski, J., Paus, S., Schild, H.H., Klockgether, T., Boecker, H., 2019. Disentangling motor planning and motor execution in unmedicated de novo Parkinson's disease patients: An fMRI study. Neuroimage Clin. 22, 101784.

Matar, E., Shine, J.M., Gilat, M., Ehgoetz Martens, K.A., Ward, P.B., Frank, M.J., Moustafa, A.A., Naismith, S.L., Lewis, S.J.G., 2019. Identifying the neural correlates of doorway freezing in Parkinson's disease. Hum. Brain Mapp. 40, 2055–2064.

Mayka, M.A., Corcos, D.M., Leurgans, S.E., Vaillancourt, D.E., 2006. Three-dimensional locations and boundaries of motor and premotor cortices as defined by functional brain imaging: a meta-analysis. Neuroimage 31, 1453–1474.

Meder, D., Herz, D.M., Rowe, J.B., Lehéricy, S., Siebner, H.R., 2019. The role of dopamine in the brain – lessons learned from Parkinson's disease. Neuroimage 190, 79–93.

Nasreddine, Z.S., Phillips, N.A., Bédirian, V., Charbonneau, S., Whitehead, V., Collin, I., Cummings, J.L., Chertkow, H., 2005. The Montreal Cognitive Assessment, MoCA: A Brief Screening Tool For Mild Cognitive Impairment. J. Am. Geriatr. Soc. 53, 695–699.

Neely, K.A., Kurani, A.S., Shukla, P., Planetta, P.J., Shukla, A.W., Goldman, J.G., Corcos, D.M., Okun, M.S., Vaillancourt, D.E., 2015. Functional Brain Activity Relates to 0–3 and 3–8 Hz Force Oscillations in Essential Tremor. Cereb. Cortex 25, 4191–4202.

Niethammer, M., Feigin, A., Eidelberg, D., 2012. Functional neuroimaging in Parkinson's disease. Cold Spring Harb. Perspect. Med. 2, a009274.

Obeso, J.A., Stamelou, M., Goetz, C.G., Poewe, W., Lang, A.E., Weintraub, D., Burn, D., Halliday, G.M., Bezard, E., Przedborski, S., Lehericy, S., Brooks, D.J., Rothwell, J.C., Hallett, M., DeLong, M.R., Marras, C., Tanner, C.M., Ross, G.W., Langston, J.W., Klein, C., Bonifati, V., Jankovic, J., Lozano, A.M., Deuschl, G., Bergman, H., Tolosa, E., Rodriguez-Violante, M., Fahn, S., Postuma, R.B., Berg, D., Marek, K., Standaert, D.G., Surmeier, D.J., Olanow, C.W., Kordower, J.H., Calabresi, P., Schapira, A.H.V., Stoessl, A.J., 2017. Past, present, and future of Parkinson's disease: A special essay on the 200th Anniversary of the Shaking Palsy. Mov. Disord. 32, 1264–1310.

Pinto, S., Mancini, L., Jahanshahi, M., Thornton, J.S., Tripoliti, E., Yousry, T.A., Limousin, P., 2011. Functional magnetic resonance imaging exploration of combined hand and speech movements in Parkinson's disease. Mov. Disord. 26, 2212–2219.

Piramide, N., Agosta, F., Sarasso, E., Canu, E., Volontè, M.A., Filippi, M., 2020. Brain activity during lower limb movements in Parkinson's disease patients with and without freezing of gait. J. Neurol. 267, 1116–1126.

Planetta, P.J., Kurani, A.S., Shukla, P., Prodoehl, J., Corcos, D.M., Comella, C.L., McFarland, N.R., Okun, M.S., Vaillancourt, D.E., 2015. Distinct functional and macrostructural brain changes in Parkinson's disease and multiple system atrophy. Hum. Brain Mapp. 36, 1165–1179.

Poewe, W., Seppi, K., Tanner, C.M., Halliday, G.M., Brundin, P., Volkmann, J., Schrag, A.-E., Lang, A.E., 2017. Parkinson disease. Nat. Rev. Disease Primers 3, 17013.

Power, J.D., Barnes, K.A., Snyder, A.Z., Schlaggar, B.L., Petersen, S.E., 2012. Spurious but systematic correlations in functional connectivity MRI networks arise from subject motion. Neuroimage 59, 2142–2154.

Prodoehl, J., Yu, H., Little, D.M., Abraham, I., Vaillancourt, D.E., 2008. Region of interest template for the human basal ganglia: comparing EPI and standardized space approaches. Neuroimage 39, 956–965.

Prodoehl, J., Spraker, M., Corcos, D., Comella, C., Vaillancourt, D., 2010. Blood oxygenation level-dependent activation in basal ganglia nuclei relates to specific symptoms in de novo Parkinson's disease. Mov. Disord. 25, 2035–2043.

Pyatigorskaya, N., Gallea, C., Garcia-Lorenzo, D., Vidailhet, M., Lehericy, S., 2014. A review of the use of magnetic resonance imaging in Parkinson's disease. Ther. Adv. Neurol. Disord. 7, 206–220.

Sabatini, U., Boulanouar, K., Fabre, N., Martin, F., Carel, C., Colonnese, C., Bozzao, L., Berry, I., Montastruc, J.L., Chollet, F., Rascol, O., 2000. Cortical motor reorganization in akinetic patients with Parkinson's disease: a functional MRI study. Brain 123 (Pt 2), 394–403.

Sarasso, E., Gardoni, A., Piramide, N., Volontè, M.A., Canu, E., Tettamanti, A., Filippi, M., Agosta, F., 2021. Dual-task clinical and functional MRI correlates in Parkinson's disease with postural instability and gait disorders. Parkinsonism Relat. Disord. 91, 88–95.

Schwingenschuh, P., Katschnig, P., Jehna, M., Koegl-Wallner, M., Seiler, S., Wenzel, K., Ropele, S., Langkammer, C., Gattringer, T., Švehlík, M., Ott, E., Fazekas, F.,

Schmidt, R., Enzinger, C., 2012. Levodopa changes brain motor network function during ankle movements in Parkinson's disease. J. Neural Transm. 120, 423–433.

Shine, J.M., Matar, E., Ward, P.B., Bolitho, S.J., Gilat, M., Pearson, M., Naismith, S.L., Lewis, S.J., 2013. Exploring the cortical and subcortical functional magnetic resonance imaging changes associated with freezing in Parkinson's disease. Brain 136, 1204–1215.

Solstrand Dahlberg, L., Lungu, O., Doyon, J., 2020. Cerebellar Contribution to Motor and Non-motor Functions in Parkinson's Disease: A Meta-Analysis of fMRI Findings. Front. Neurol. 11.

Spraker, M.B., Prodoehl, J., Corcos, D.M., Comella, C.L., Vaillancourt, D.E., 2010. Basal ganglia hypoactivity during grip force in drug naïve Parkinson's disease. Hum. Brain Mapp. 31, 1928–1941.

Sterling, N.W., Lewis, M.M., Du, G., Huang, X., 2016. Structural Imaging and Parkinson's Disease: Moving Toward Quantitative Markers of Disease Progression. J. Parkinsons Dis. 6, 557–567.

Tzourio-Mazoyer, N., Landeau, B., Papathanassiou, D., Crivello, F., Etard, O., Delcroix, N., Mazoyer, B., Joliot, M., 2002. Automated anatomical labeling of activations in SPM using a macroscopic anatomical parcellation of the MNI MRI single-subject brain. Neuroimage 15, 273–289.

Upton, J., 2013. Beck Depression Inventory (BDI). In: Gellman, M.D., Turner, J.R. (Eds.), Encyclopedia of Behavioral Medicine. Springer, New York, New York, NY, pp. 178–179.

Wu, T., Hallett, M., 2013. The cerebellum in Parkinson's disease. Brain 136, 696–709.

Wu, T., Wang, L., Hallett, M., Li, K., Chan, P., 2010. Neural correlates of bimanual anti-phase and in-phase movements in Parkinson's disease. Brain 133, 2394–2409.